Reactive and Functional Polymers 195 (2024) 105825

Contents lists available at ScienceDirect

Reactive and Functional Polymers

journal homepage: www.elsevier.com/locate/react

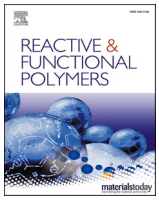

Perspective Article

Harnessing disulfide and transesterification bond exchange reactions for recyclable and reprocessable 3D-printed vitrimers

Anna Vilanova-Pérez [a], Sasan Moradi [a], Osman Konuray [a], Xavier Ramis [a], Adrià Roig [b,*], Xavier Fernández-Francos [a,*]

[a] Universitat Politècnica de Catalunya, Thermodynamics Laboratory, ETSEIB, Av. Diagonal, Barcelona 08028, Spain
[b] Universitat Rovira i Virgili, Department of Analytical and Organic Chemistry, C/ Marcel·lí Domingo 1, Edif. N4, Tarragona 43007, Spain

ARTICLE INFO

Keywords:
Vitrimer
Disulfide metathesis
Transesterification
3D-printing
Recyclability

ABSTRACT

Two new vitrimeric materials have been studied for potential additive manufacturing applications such as 3D-printing. A monomer containing disulfide bonds and β-hydroxyesters was easily synthesized from two low-cost and commercially available reagents. Another disulfide-containing monomer was synthesized for comparison purposes. Materials were prepared through a UV-light radical polymerization of methacrylates. The addition of two reactive diluents such as poly(ethylene glycol) methyl ether methacrylate (PEGMA) and ethylene glycol phenyl ether methacrylate (EGPMA) was necessary to achieve a suitable viscosity for the curing as well as for their printability. The curing process was controlled by FTIR. Thermomechanical properties were investigated by means of DMTA analysis revealing near-ambient T_g values. Stress relaxation tests revealed that both materials were capable to relax the 63% of the initial stress in less than 10 min at 110 °C. The recyclability of the materials was achieved, and the mechanical and thermomechanical properties of the recycled samples were compared to the virgin ones revealing a great recovery of the initial properties. Finally, Digital Light Processing (DLP) technique was used to print complex structures with high resolution highlighting the great potential of these vitrimeric materials in 3D printing.

1. Introduction

Nowadays, the generation of waste is one of the current challenges concerning the polymer industry. In this field, thermosetting materials are widely used in several daily life applications thanks to their good mechanical performance and their high chemical and solvent resistance [1]. However, their crosslinked structure impedes recyclability and reprocessability, thus producing huge environmental issues. Nevertheless, the incorporation of dynamic bonds in the polymer network enables reversible chemical reactions when an external stimulus, such as heat or UV light, is applied, thereby constituting a promising solution for the problem of thermoset waste management [2]. These covalent adaptable networks (CANs) can behave as thermosets at specific temperatures but when they are subjected to a stimulus, they are able to change from a viscoelastic solid-like to a fluid-like plastic behavior which enables reshapeability, self-repair or recyclability like thermoplastics [3]. Depending on the exchange mechanism of the reversible chemical reactions, CANs are divided into two main groups: dissociative and associative. The former group relies on a two-step mechanism, wherein a bond is firstly broken, to be reformed later at a different location. This produces a loss of crosslinking density and therefore, a sudden drop of viscosity upon heating. The latter group, on the other hand, maintains the crosslinking density while flowing, producing a gradual decrease of viscosity upon heating, following an Arrhenius-type dependence like inorganic vitreous silica [4]. For this reason, these materials are called vitrimers and were first described by Liebler and co-workers in 2011.

Since then, many organic reactions such as transesterification [5,6] transamination of vinylogous urethanes [7,8], imine metathesis [9,10], olefine metathesis [11,12] and disulfide metathesis [13,14] have been exploited for the synthesis of vitrimeric materials. Among this large and inexhaustive set of bond exchange reactions, disulfide metathesis stands out with the outstanding self-healing and/or self-welding capabilities it bestows to the polymeric materials possessing disulfide bonds. Exploiting this unique chemistry in macromolecules is therefore crucial for the advanced plastics industry which relies heavily in thermosets [15,16].

In recent years, additive manufacturing (more commonly known as

* Corresponding authors.
E-mail addresses: adria.roig@urv.cat (A. Roig), xavier.fernandez@upc.edu (X. Fernández-Francos).

https://doi.org/10.1016/j.reactfunctpolym.2023.105825
Received 18 September 2023; Received in revised form 23 December 2023; Accepted 29 December 2023
Available online 4 January 2024

3D printing) technologies have gained momentum as the industrial paradigms evolve towards customization-based and fast throughput processes. The product versatility and customizability coupled with the processing speed of 3D printing methods have found them a widespread applicability across many industrial fields [17,18]. Nowadays, many thermoplastic and thermosetting materials can be processed using different 3D printing methodologies. For their aforementioned advantages, vitrimers or vitrimer-like materials are also being used more and more in 3D printing applications [19–21]. In this context, many researchers have focused their attention on the use of photosensitive resins which contain dynamic bonds in their formulations [22,23]. As an example, Shi et al. [24] present an epoxy-based thermoset vitrimer with dynamic β-hydroxy esters that can undergo a reversible transesterification reaction. After precuring the ink at 130 °C to get a high viscosity prepolymer, they print complex 3D structures at high temperatures via direct ink writing (DIW). Importantly, materials can be chemically recycled with ethylene glycol and can be reused. They successfully show 4 reprocessing cycles without loss of mechanical properties. More recently, our group described 3D-printed acrylate-epoxy hybrid networks with different concentrations of dynamic β-hydroxy esters [25]. All the materials could be tailored by changing the proportions and loadings of the starting monomers thereby yielding a large set of thermomechanical, tensile, and vitrimeric properties. We also demonstrated the printability of the resins by making use of Digital Light Processing (DLP) methodology as well as showing the recyclability of the materials with full recovery of tensile properties.

There are other dynamic bonds that have been proven suitable for developing vitrimeric materials for 3D printing. Zhao and *co*-workers reported the successful synthesis of a polyurethane acrylate containing disulfide bonds that can be processed via DLP 3D printing to obtain complex structures with desirable properties [26]. Besides presenting outstanding elastomeric properties in the tensile test, a healing efficiency of 95% is recorded after 12 h at 80 °C up to 3 times. Later on, Stouten et al. synthesized a set of three vitrimers based on a dimer fatty acid and vanillin [27]. Their material has a bio-based content of at least 70% as well as containing a high amount of imine bonds which allow acceptably low relaxation times. Moreover, the materials can be recycled by grinding and hot-pressing for 5 min at 150 °C yielding materials with similar thermomechanical properties in comparison to the original ones.

Considering all of this, we describe two different polymer networks obtained from two different synthetic dimethacrylates possessing disulfide bonds. The monomers reacted through radical polymerization of methacrylates to yield the crosslinked materials. The in-house synthesized methacrylates were mixed with certain proportions of two commercially available methacrylates, namely poly(ethylene glycol) methyl ether methacrylate (PEGMA) and ethylene glycol phenyl ether methacrylate (EGPMA). While the former provides flexibility and mobility to the polymer network, the latter contains an aromatic ring which imparts rigidity. This particular composition of monomers allows proper viscosity adjustment, facilitating the formulation of UV-DLP printing resins. Complex geometries are 3D-printed easily with these resins. Furthermore, dynamic β-hydroxy esters (able to undergo transesterification) and disulfide bonds (able to undergo disulfide metathesis) are incorporated into the polymer matrix to allow for vitrimeric behavior. By changing the composition of materials, the relative influence of each exchange reaction can be tuned. Besides an extensive characterization of the thermal and thermomechanical properties of the cured materials, tensile tests of the virgin and recycled samples were performed to demonstrate the effectiveness of the recycling process.

2. Experimental part

2.1. Materials

The following chemicals were purchased from Sigma Aldrich: 4–4′-dithiodibutyric acid (DTBA), glycidyl methacrylate (GMA), tetramethylpiperidinooxy (TEMPO), triethanolamine (TEA), candida antarctica lipase B (CALB), methyl methacrylate (MA), poly(ethylene glycol) methyl ether methacrylate (280–320 g/mol, PEGMA), ethylene glycol phenyl ether methacrylate (EGPMA), 1,5,7-triazabicyclo[4.4.0]dec-5-ene (TBD). The photoinitiator diphenyl(2,4,6-trimethyl benzoyl) phosphine oxide (TPO) has been supplied by Ciba Specialty Chemicals Inc. Bis(2-hydroxyethyl) disulfide (HES) was obtained from ThermoFisher Scientific. T-butanol (t-BuOH), and methyl t-butyl ether (MtBE) from Scharlau. All the reagents have been used without further purification.

2.2. Characterization techniques

NMR spectroscopy. ^{1}H NMR and ^{13}C NMR spectra were recorded on a Varian VNMR-S400 NMR spectrometer. $CDCl_3$ was used as a solvent. All chemical shifts are quoted on the δ scale in part per million (ppm) using the residual protonated solvent as the internal standard (^{1}H NMR: $CDCl_3 = 7.26$ ppm; ^{13}C NMR: $CDCl_3 = 77.16$ ppm).

FTIR spectrometry. A Brucker Vertex 70FTIR spectrometer equipped with an attenuated total reflection (ATR) accessory which is temperature controlled was used to follow the curing process. The spectra were collected at room temperature in absorbance mode with a resolution of 4 cm^{-1} and a wavelength range from 600 to 4000 cm-^{1}, averaging 20 scans for each spectrum and analyzed using the OPUS software.

DSC analysis. Differential Scanning Calorimetry (DSC) was carried out with a Mettler DSC3+ calorimeter equipped with an intra-cooler and used for the determination of the glass transition temperature (T_g) after the UV-curing and the presence of residual heat. Samples of approximately 10 mg were placed in aluminum pans with pierced lids and analyzed at 10 °C·min^{-1} under a nitrogen atmosphere. The T_g was determined as the halfway point in the heat capacity step using the ISO method from the STARe software.

DMA analysis. For thermomechanical analysis, a TA Instruments DMA Q800 device was used. Prismatic samples with dimensions of 10 × 10 × 1 mm^3 (free length x width x thickness) were analyzed using a single cantilever clamp at a frequency of 1 Hz and 0.05% strain at 3 °C·min^{-1}. The T_g was determined from the temperature of the tan δ peak corresponding to the α-relaxation of the material. Stress relaxation tests were performed using a 3-point bending clamp with a preload force of 0.01 N and 1% strain. Sample dimensions were 20 × 10 × 1 mm^3 (free length x width x thickness). Samples were heated at 10 °C·min^{-1} up to the desired temperature and stabilized at that temperature, held isothermally for 5 min prior to the application of the strain and measurement of the stress as a function of time. The relaxation-stress E(t) was normalized by the initial stress E_0, and the relaxation times (τ) were determined as the time necessary to relax 0.37E_0, i.e. ($E = 1/eE_0$). With the relaxation times obtained at each temperature, the activation energy values (E_a) were calculated using an Arrhenius-type equation (Eq. (1)):

$$ln(\tau) = \frac{E_a}{RT} - lnA \quad (1)$$

where τ is the time needed to attain a given stress-relaxation value, A is the pre-exponential factor, and R is the gas constant. From Arrhenius relaxation, the topology freezing temperature (T_v) was obtained as the temperature at which the material reaches a viscosity (η) of 10^{12} Pa·s. Using the Maxwell relation (Eq. (2)) and E' determined from DMTA (assuming E' is relatively invariant in the rubbery state), τ* could be determined for each material. Then, Arrhenius relationship was extrapolated to the corresponding value of τ* to determine T_v for each

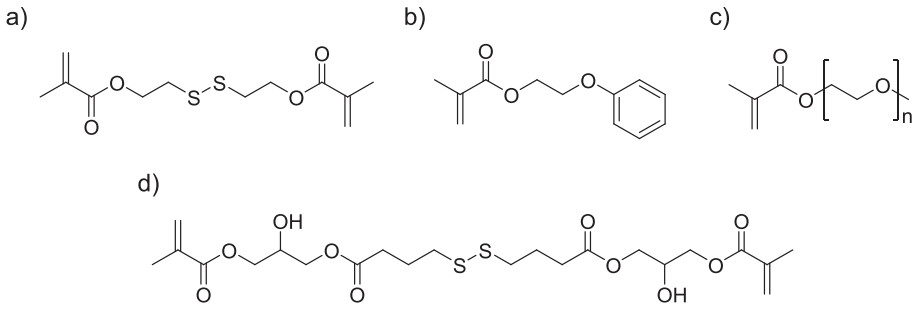

Scheme 1. Structures of a) MES, b) EGPMA, c) PEGMA, and d) S2MA.

sample.

$$\tau^* = \frac{\eta}{E'_{rubbery}} \quad (2)$$

Tensile tests. Tensile tests were performed in the same DMA device using the same sample dimensions and preload force with a ramp of 3 $N \cdot min^{-1}$.

TGA analysis. Thermogravimetric analysis (TGA) was performed using a Mettler TGA/SDTA 851e/LF/1100 thermobalance. Fully cured samples were analyzed under isothermal conditions at 120 °C and dynamic conditions at a heating rate of 10 $°C \cdot min^{-1}$. Both isothermal and dynamic scans were performed under a nitrogen atmosphere. The recycling of finely chopped samples was performed using a Specac Atlas manual 15 T hydraulic hot-press.

2.3. Preparation of S2MA

GMA (5 g, 35.2 mmol), DTBA (4.2 g, 17.6 mmol), and TEA (23 mg, 0.15 mmol) were weighted in a 20 mL vial equipped with a magnetic stirrer followed by the addition of TEMPO (23 mg, 0.15 mmol) as a radical scavenger. Then, the vial was placed at 100 °C until complete dissolution of the acid. Finally, the vial was wrapped in aluminum foil, put at 80 °C, to prevent premature activation of the radical polymerization of the methacrylate, and kept for 4 h until the completion of the reaction. S2MA was then obtained as a viscous yellowish liquid and was used without any purification.

^{1}H NMR ($CDCl_3$, δ in ppm): 1.19 (s, 3H); 1.96 (tt, 2H); 2.43 (t, 2H); 2.67 (t, 2H); 4.41–3.49 (m, 6H); 6.55 (s, 1H); 6.09 (s, 1H) (Fig. S1).

^{13}C NMR ($CDCl_3$ δ in ppm): 18.20; 24.60; 28.90; 34.01; 65.10; 65.41; 68.19; 126.29; 135.87; 167.90; 173.70 (Fig. S2).

2.4. Preparation of MES

The use of MES was previously described elsewhere [28], but a different methodology to synthesize it was used herein. In a 100 mL two-necked round-bottom flask equipped with a magnetic stirrer and a soxhlet system with glass wool, activated 4 Å molecular sieves, and a condenser, HES (2 g, 13 mmol) was weighted and dissolved in 60 mL of MtBE/tert-butanol (70/30 *v*/v). Then, MA (11.7 mL, 0.13 mol) was added, the mixture heated until reflux (80 °C) and the soxhlet drained 4 times. Next, CALB (150 mg, 7.5% *w*/w to HES) was added, and the reaction was kept for 6 h at the same temperature. Finally, the mixture was vacuum-filtered, and the solvent evaporated in a rotary evaporator yielding MES as a colorless liquid (85%).

^{1}H NMR ($CDCl_3$, δ in ppm): 1.87 (s, 3H); 2.90 (t, 2H); 4.34 (t, 2H); 5.52 (s, 1H); 6.06 (s, 1H) (Fig. S3).

^{13}C NMR ($CDCl_3$ in δ ppm): 17.90; 37.30; 62.50; 126.0; 136.0; 167.1. (Fig. S4).

2.5. Sample preparation

In Scheme 1, the structures of the most important reagents used in sample preparation are collected. All the formulations were prepared by mixing a 25% (*w*/w) of either S2MA or MES and a 75% (w/w) of a mixture 50/50 (w/w) of EGPMA/PEGMA. Then, 2 phr of TPO (radical photoinitiator) and 3 phr of TBD were added to the mixture and manually stirred until complete homogeneity. Each liquid formulation was injected into a rectangular mold made of two microscope slides sandwiching a spacer made of Teflon of 1 mm of thickness with the desired shape. The samples were photocured for 15 min in a Photopol Vacuum UV oven with an irradiation density of 1 W/cm^2. Samples were encoded as PolyX, where X refers to the name of the dimethacrylate monomer. Table 1 details the composition of both vitrimeric materials prepared herein.

Table 1
Composition of the vitrimeric materials prepared.

Sample	S2MA (w/w)	MES (w/w)	EGPMA (w/w)	PEGMA (w/w)	TPO (phr)	TBD (phr)
PolyS2MA	25	–	37.5	37.5	2	3
PolyMES	–	25	37.5	37.5	2	3

2.6. DLP printing

3D-printing of objects with complex geometries was performed using both PolyS2MA and PolyMES as printing resins. An Asiga Max UV 385 DLP printer was used (bottom-up configuration) with an irradiation wavelength of 385 nm (UV region). The printing parameters were chosen based on the relation between irradiation intensity and cure depth (characterized by Jacobs working curves, the one for PolyS2MA given in Fig. S5, supporting information). As the slice thickness was chosen as 100 μm, irradiation time was set as 4 s, with the first layer irradiated for 8 s (base layer) at an irradiation intensity of 5.93 mW/cm^2. These parameters were the same regardless of the resin as both resins had similar photocuring kinetics. These irradiation durations safely ensure a cure depth of 100 μm as can be confirmed from Fig. S5 (supporting information).

3. Results and discussion

3.1. Study of curing procedure

Both materials were obtained through a radical polymerization of methacrylic groups under UV light and using TPO as the photoinitiator. TBD was used as the catalyst for the disulfide exchange since it is reported that tertiary amines are suitable catalysts for this reaction [29–32]. Fig. S6 demonstrates the superior catalysis of TBD over other catalysts in this system. FTIR spectra of the initial formulation and the final material after UV curing were recorded to confirm the completion of the reaction (Fig. 1). As can be seen, the characteristic band of methacrylates at 1350 cm^{-1} completely disappeared upon UV irradiation (as explained in section 2.5). Moreover, the band at 1636 cm^{-1} corresponding to the stretching of the C═C bond of methacrylic groups

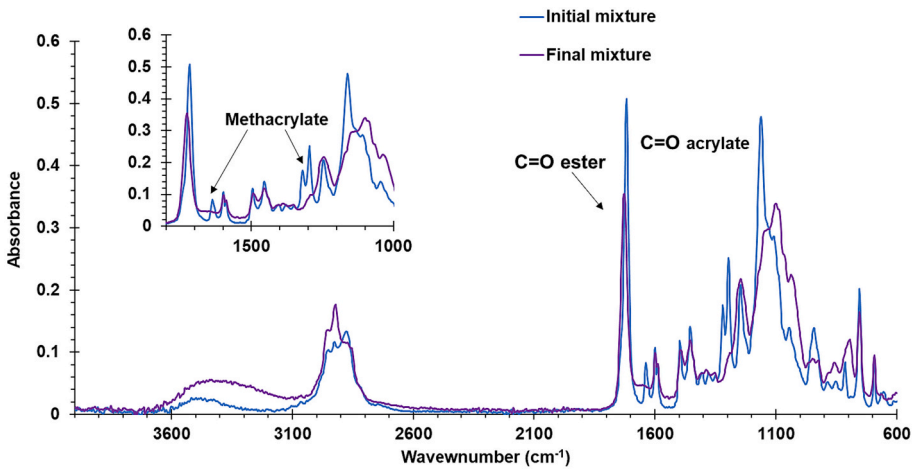

Fig. 1. FTIR spectra of the initial mixture (blue) and the final material (purple) of polyS2MA. (For interpretation of the references to colour in this figure legend, the reader is referred to the web version of this article.)

Table 2
Thermogravimetric and thermomechanical data of polyS2MA and polyMES.

Sample	T_g^{DSC} (°C)	$T_{5\%}$[a] (°C)	T_{max}[b] (°C)	Char yield[c] (%)	$T_{tan\ \delta}$[d] (°C)	E'_{glassy}[e] (MPa)	$E'_{rubbery}$[f] (MPa)
PolyS2MA	7.0	234	350	5.8	18.4	2610	4.8
PolyMES	12.0	219	354	5.7	27.1	2925	16.2

[a] Temperature of 5% of weight loss.
[b] Temperature at the maximum rate of degradation.
[c] Char residue at 600 °C.
[d] Temperature at the maximum of tan δ peak at 1 Hz.
[e] Glassy storage modulus at T_g - 50 °C by DMTA.
[f] Rubbery storage modulus at T_g + 50 °C by DMTA.

also vanished and the band corresponding to the carbonyl group experimented a slight change which suggests the formation of esters (reacted acrylates). Thus, the polymerization of methacrylates was successfully achieved confirming the completion of cure of the samples after the UV curing procedure. To characterize the materials DSC analysis of the cured samples were performed (see Fig. S7, Table 2). As it can be observed, both T_g are sub-ambient, with that of polyMES, slightly higher due to its tighter network structure. The same thermograms also confirm the completion of the cure since no exothermal peak can be observed up to 200 °C. Once the completeness of cure was established, the resins were tested in UV-DLP printing. Photographs of some complex-shaped objects printed with both PolyMES and PolyS2MA are given in Fig. 2. The printing parameters were chosen as detailed in the experimental section.

3.2. Study of the thermal and thermomechanical properties

The thermal stability of the materials was studied by thermogravimetry (TGA). Fig. 3 shows the TGA curves and their derivatives. The data extracted are collected in Table 2.

Both materials have relatively high thermal stability, losing 5% of their weight above 215 °C. The derivatives reveal two main peaks, the first of which can be ascribed to S—S bond breakage as well as the β-elimination of the esters present in both networks (around 230 °C) and the second peak (around 350 °C) is ascribed to the degradation of main chain C—C bonds [33,34]. Both materials exhibit low and similar values of char yield since the major part of the structure consists of aliphatic chains and the same proportion of EGPMA is used in both materials.

The thermomechanical properties of the materials were investigated by means of DMTA. Fig. 4 shows the evolution of tan δ and the storage modulus (E') with temperature of both materials while the data extracted are summarized in Table 2. As can be seen in the graphs, both

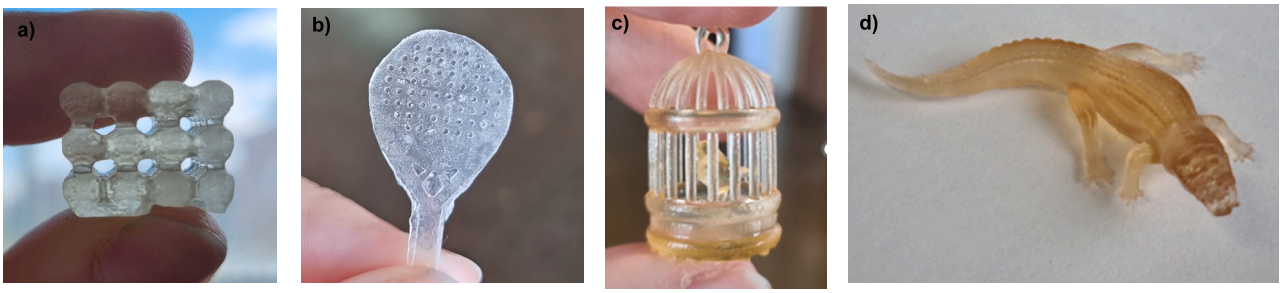

Fig. 2. A zeolitic structure (a) and a miniature tennis racket (b) printed with polyMES; a bird cage (c) and an alligator (d) printed with polyS2MA.

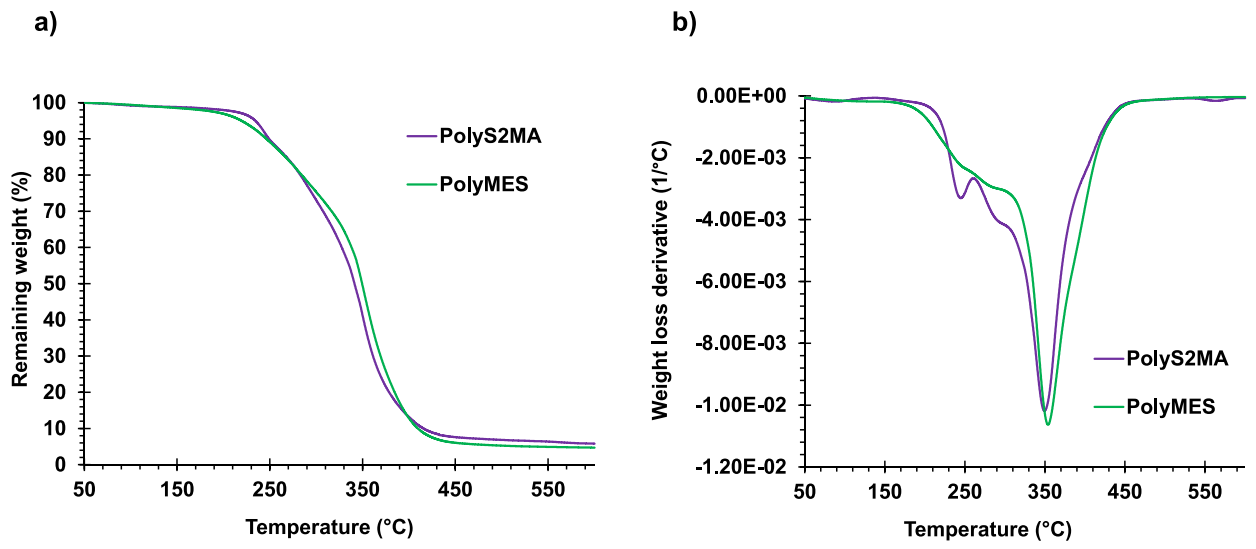

Fig. 3. (a) Thermogravimetric curves and (b) DGT curves of both materials.

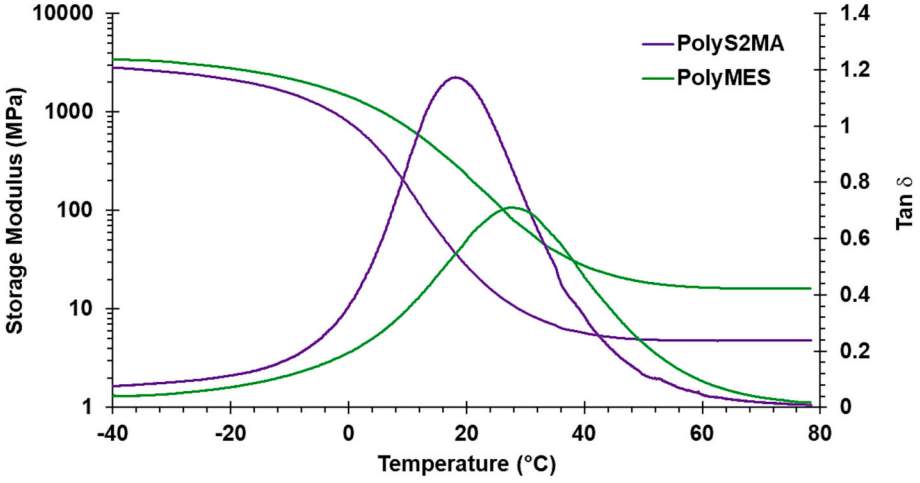

Fig. 4. Evolution of tan δ and storage modulus with temperature for both materials.

materials displayed monomodal curves which indicate the presence of a single network matrix.

Despite that S2MA and MES are used as crosslinking agents due to their high functionality, the utilization of EGPMA and PEGMA as reactive diluents decrease the T_g of the materials to 18.4 °C for polyS2MA and 27.1 °C for polyMES. In any case, the materials showed similar T_g values (taken as the maximum peak of the tan δ) around room temperature. The slightly higher T_g of polyMES was due to the shorter chain of MES that resulted in a more densely crosslinked network in comparison to that of polyS2MA. A similar trend can be observed in the storage modulus. As can be seen, polyMES showed high values of storage modulus in the glassy state resulting in a highly rigid material at low temperatures. In the case of the rubbery state, the longer chain of S2MA provided higher mobility and flexibility to the material which resulted in lower values of E', suggesting lower crosslinking density.

3.3. Study of the vitrimeric behavior

Both materials present dynamic groups able to perform bond exchange reactions upon being heated. While polyMES only contains S—S bonds that can undergo thermal disulfide metathesis, polyS2MA also contains dynamic β-hydroxyesters able to undergo transesterification reaction at high temperatures. To study this dynamicity, stress-relaxation tests at different temperatures were performed by DMTA. Fig. 5 shows the stress-relaxation curves while the main characteristic data are depicted in Table 3. As can be observed in the graphs, both materials were able to relax the 63% of the initial stress in less than 10 min even at relatively low temperatures such as 110 °C. Interestingly, polyS2MA, reaches a non-zero value of stress at the end of the relaxation while polyMES achieves a total relaxation after 100 min. It is known that transesterification processes usually occur at high temperatures while the disulfide metathesis tends to occur at lower temperatures [35]. For this reason, one may argue that the exchange kinetics of polyS2MA at such temperatures (from 110 to 140 °C) is mainly controlled by the disulfide exchange. However, at longer relaxation times, transesterification reactions could commence, leading to the formation of different structures in the polymer network. In Scheme 2, it can be observed that when a transesterification reaction occurs within the network, two different structures can result. In the first structure formed, a new additional ester acts as a crosslink between chains, so it is unlikely that the disulfide exchange breaks the connection between polymer chains completely to achieve stress relaxation. In addition, the second structure (Scheme 2, bottom) is a pendant chain, within which the occurrence of disulfide exchange would be irrelevant in terms of stress relaxation [36]. For this reason, polyS2MA did not achieve a complete relaxation or may need longer time and/or higher

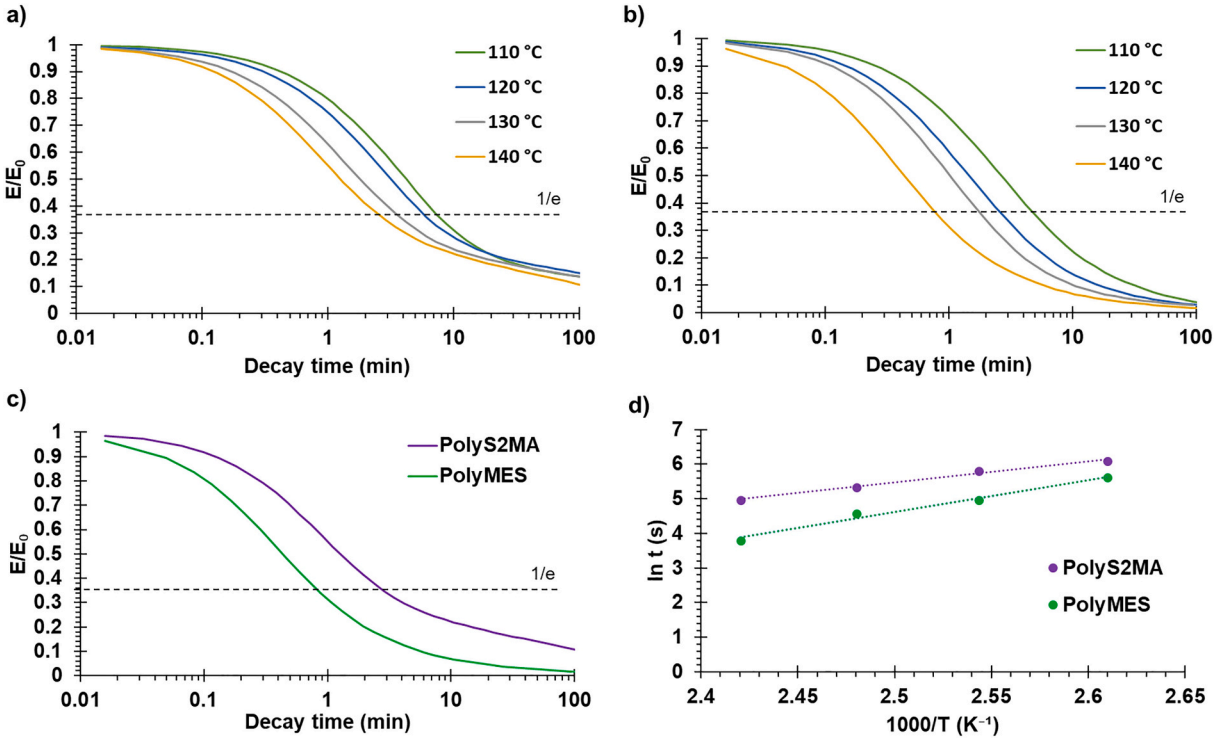

Fig. 5. Normalized stress relaxation plots as a function of time at different temperatures for (a) polyS2MA and (b) polyMES samples (c) comparison of both materials at 140 °C (d) Arrhenius plot of relaxation times against temperature for both materials.

Table 3
Relaxation times, topology freezing temperature, activation energy, and adjusting parameters for the Arrhenius equation of both samples prepared.

Sample	$\tau_{0.37}$ (min)[a]	T_v (°C)	E_a (kJ mol^{-1})	ln A (s)	R^2
PolyS2MA	2.38	21.4	50.5	10.9	0.99
PolyMES	0.74	45.4	76.8	10.5	0.98

[a] Time to reach value of $E/E_0 = 0.37$ at 140 °C.

temperatures.

An Arrhenius-type temperature dependence is exhibited by vitrimeric materials which represents a temperature-viscosity relationship similar to that of inorganic silica materials [4]. To further investigate the vitrimeric behavior of our materials, the times required to relax the 63% of the initial stress ($E/E_0 = 0.37$) at different temperatures were obtained from the relaxation curves and fitted to an Arrhenius-type equation. The resulting data allowed the calculation of the activation

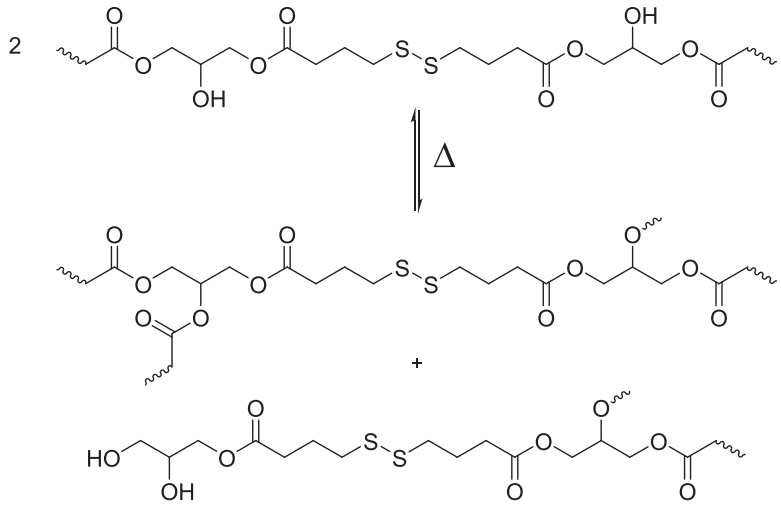

Scheme 2. Possible structures resulting from the transesterification of polyS2MA.

Table 4
Thermomechanical data of the virgin and recycled materials.

Sample	$T_{tan\ \delta}$ [a] (°C)	E'_{glassy} [b] (MPa)	$E'_{rubbery}$ [c] (MPa)	E' (MPa)	ε_{break} (MPa)	σ_{break} (MPa)
PolyS2MA virgin	18.4	2610	4.8	5.5 ± 1.8	54.3 ± 12.5	2.5 ± 0.6
PolyS2MA recycled 4 h	14.1	3610	2.7	2.8 ± 0.7	33.1 ± 8.4	0.9 ± 0.4
PolyS2MA recycled 24 h	24.2	3093	2.8	3.7 ± 0.7	51.4 ± 9.6	2.1 ± 0.2
PolyMES virgin	27.1	2925	16.2	15.6 ± 4.4	24.5 ± 0.4	3.9 ± 2.7
PolyMES recycled 4 h	29.7	2814	8.2	11.9 ± 3.6	24.3 ± 1.2	3.0 ± 0.9

[a] Temperature at the maximum of tan δ peak at 1 Hz.
[b] Glassy storage modulus at T_g - 50 °C determined by DMTA.
[c] Rubbery storage modulus at T_g + 50 °C determined by DMTA.

energy (E_a) of the exchange reactions (Fig. 5d and Table 3) for both materials. As can be seen, polyMES showed a higher E_a value, indicating the strong temperature dependence of the exchange kinetics. Nevertheless, despite the high rigidity and the high crosslinking density of the obtained materials, the E_a values were significantly lower than those obtained for other vitrimeric materials such as polyester vitrimers (90 kJ mol^{-1}), poly(urethane) dynamic networks (130 kJ mol^{-1}), or even aromatic disulfide materials (99–357 kJ mol^{-1}) [30,37,38].

Another important parameter for vitrimeric materials is the topology freezing temperature (T_v) which is defined as the temperature below which the exchange reactions are almost negligible. In practical terms, it is generally accepted that this corresponds to the temperature at which the material achieves a viscosity of 10^{12} Pa·s. Both T_v were calculated by making use of the Maxwell relationship and an extrapolation of the relaxation curves (see Table 3). Despite the lower values of T_v of the materials, both were slightly higher than their corresponding T_g. Similar to the comparison of their T_g, polyMES had a higher T_v. Even though disulfide exchange tends to occur at lower temperatures than transesterification [35], polyMES requires a higher temperature to initiate the exchange reactions (higher T_v) in comparison to polyS2MA probably due to its higher crosslinking density (as demonstrated by its higher $E'_{rubbery}$, see Table 2), which results in a lower chain mobility.

3.4. Mechanical recycling

The most practically relevant property of any vitrimeric material is its recyclability and reprocessability. The recycling capabilities of the materials were tested by chopping them into small pieces and then hot-pressing in a mechanical press under 5 MPa. The recycling temperature was set to 120 °C for both materials to ensure that the exchange reactions take place. After the recycling process, transparent samples could be obtained, suggesting good homogeneity but, due to the high content of permanent bonds in the structure, small defects could be observed (Fig. S8). Moreover, to ensure that 120 °C is a safe temperature for recycling (without any thermal degradation), a thermogravimetric study was carried out at 120 °C for a residence time of 4 h. Fig. S9 shows that neither material degrades more than 3% during this time, indicating that the network integrity is maintained. In the case of polyS2MA, it was not possible to achieve a homogenous sample after 4 h probably due to its inability to completely relax stress. As a result, the recycling time was increased to 24 h for this material. After this, an improvement of the recycled sample can be appreciated (Fig. S8). DMTA tests were performed to compare the thermomechanical properties of the recycled polyS2MA and polyMES materials with their virgin counterparts. Fig. 5 shows the evolution of the storage modulus and the tan δ with the temperature and Table 4 summarizes the important data from these

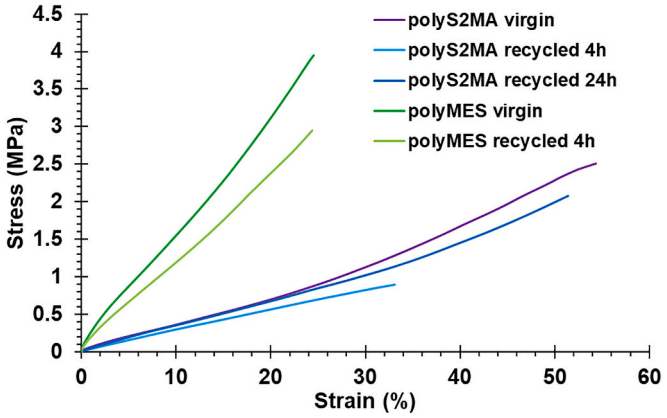

Fig. 7. Stress-strain curves of the original and recycled samples of polyS2MA and polyMES.

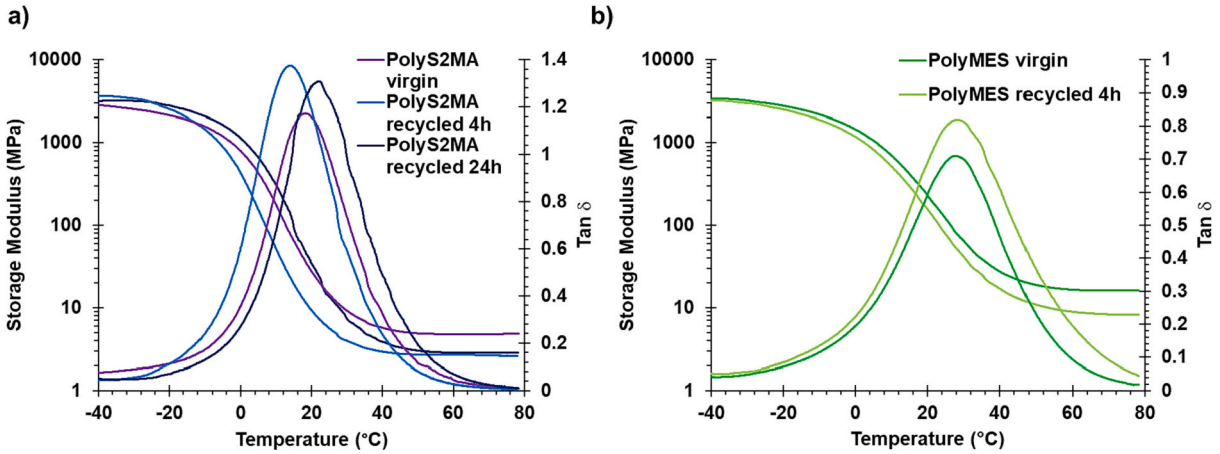

Fig. 6. Evolution of tan δ and storage modulus with temperature before and after recycling of (a) polyS2MA and (b) polyMES.

analyses.

As can be seen, similar tan δ curves and $T_{\tan\delta}$ values were obtained in both cases. In the case of polyS2MA, slight differences can be observed between the 4 h and 24 h recycled samples. The 4 h recycled polyS2MA material showed lower $T_{\tan\delta}$ values in comparison to the virgin sample, suggesting the inadequacy of the recycling process. This is probably due to the fact that this material failed to reach complete relaxation within 4 h (see Fig. 6a). However, the 24 h recycled material seems to have recovered most of its $T_{\tan\delta}$. Caution should be given to the possibility that during recycling some covalent bonds were broken within the network which would lead to slight decreases in viscoelastic properties (e.g., rubbery state storage modulus). However, the results suggest that the materials could be safely recycled without significant changes in their thermomechanical behavior.

Moreover, to evaluate and compare the mechanical properties of the virgin and recycled polyS2MA and polyMES materials, stress-strain tests were performed with DMTA at 30 °C. As shown in Fig. 7 and Table 4, the results obtained for the virgin and recycled samples are comparable. Similar values of tensile modulus, stress at break and strain at break confirmed successful recycling of both vitrimeric materials. The 4 h recycled polyS2MA sample displayed lower values of stress and strain at break, similar to the deterioration of viscoelastic performance observed earlier.

4. Conclusions

Two new UV-curable vitrimeric materials have been successfully synthesized from cheap and commercially available reagents. To improve the processability and recyclability of the UV-cured final polymers, ethylene glycol phenyl ether methacrylate (EGPMA) and poly (ethylene glycol) methyl ether methacrylate (PEGMA) were employed as reactive diluents. Final materials were characterized with respect to their viscoelastic properties, stress relaxation capabilities, as well as their mechanical properties before and after recycling.

Both materials exhibit near-ambient T_g, with that of poly(MES) being slightly higher as it has a more densely crosslinked structure.

The materials exhibit excellent vitrimeric behavior with characteristic relaxation times of less than 2.5 min at 140 °C with a catalyst load of only 3 phr. Stress relaxation behavior of the materials could be modelled by an Arrhenius-type relationship, yielding activation energies (E_a) that were significantly lower than previously reported vitrimeric polymers. The topology freezing temperatures followed the same trend as the T_g; polyMES showed a higher T_v than polyS2MA. Although disulfide exchange could happen at lower temperatures than transesterification reaction, due to the higher crosslinking density of polyMES, a higher temperature is required to increase the chains' mobility and facilitate the interchange. Nevertheless, in both materials, T_v values were higher than T_g values suggesting the possibility of complex shape-memory programming (not treated in this work).

Moreover, the recyclability of the materials was assessed by grinding and hot-pressing them at 120 °C. Hot-pressing was continued for a longer time in the case of polyS2MA as it was observed that the exchange reactions within this material took longer to reach equilibrium. The thermomechanical properties of the original and the recycled materials were highly similar thereby proving the success of our recycling procedures. Furthermore, recycled materials successfully recovered their Young's moduli, stress at break and strain at break values.

Both formulations could be easily and rapidly 3D-printed using a DLP printer to obtain complex shapes with relatively high resolution, putting in evidence the potential application of these vitrimeric materials in additive manufacturing industry.

CRediT authorship contribution statement

Anna Vilanova-Pérez: Writing – original draft, Investigation. **Sasan Moradi:** Investigation. **Osman Konuray:** Writing – review & editing, Methodology. **Xavier Ramis:** Writing – review & editing, Funding acquisition. **Adrià Roig:** Writing – review & editing, Supervision, Investigation. **Xavier Fernández-Francos:** Writing – review & editing, Supervision, Conceptualization.

Declaration of competing interest

There is no conflict of interests to declare.

Data availability

Data will be made available on request.

Acknowledgments

This work was funded by the Spanish Ministry of Science and Innovation (MCIN/AEI/10.13039/501100011033) through R&D projects PID2020-115102RB-C21 and PID2020-115102RB-C22, and also by Generalitat de Catalunya (2021-SGR-00154 and BASE3D). X. Fernández-Francos and O. Konuray acknowledge the Serra-Húnter programme (Generalitat de Catalunya).

Appendix A. Supplementary data

Structural characterization of the monomers, preliminary stress relaxation tests, calorimetry, thermogravimetry and photographs of the recycled samples. Supplementary data to this article can be found online at [https://doi.org/10.1016/j.reactfunctpolym.2023.105825].

References

[1] J.P. Pascault, H. Sautereau, J. Verdu, R.J.J. Wiliams, Thermosetting Polymers, Marcel Dekker, New York, 2002.
[2] M. Podgórski, B.D. Fairbanks, B.E. Kirkpatrick, M. McBride, A. Martinez, A. Dobson, N.J. Bongiardina, C.N. Bowman, Toward stimuli-responsive dynamic thermosets through continuous development and improvements in covalent adaptable networks (CANs), Adv. Mater. 32 (2020) 1906876–1906902, https://doi.org/10.1002/adma.201906876.
[3] P. Chakma, D. Konkolewicz, Dynamic covalent bonds in polymeric materials, Angew. Chem. Int. Ed. 131 (2019) 9784–9797, https://doi.org/10.1002/anie.201813525.
[4] W. Denissen, J.M. Winne, F.E. Du Prez, Vitrimers: permanent organic networks with glass-like fluidity, Chem. Sci. 7 (2016) 30–38, https://doi.org/10.1039/c5sc02223a.
[5] F.I. Altuna, C.E. Hoppe, R.J.J. Williams, Epoxy vitrimers with a covalently bonded tertiary amine as catalyst of the transesterification reaction, Eur. Polym. J. 113 (2019) 297–304, https://doi.org/10.1016/j.eurpolymj.2019.01.045.
[6] M. Capelot, D. Montarnal, F. Tournilhac, L. Leibler, Metal-catalyzed transesterification for healing and assembling of thermosets, J. Am. Chem. Soc. 134 (2012) 7664–7667, https://doi.org/10.1021/ja302894k.
[7] E. Manarin, F. Da Via, B. Rigatelli, S. Turri, G. Griffini, Bio-based vitrimers from 2,5-furandicarboxylic acid as repairable, reusable, and recyclable epoxy systems, ACS Appl. Polym. Mater. 5 (2023) 828–838, https://doi.org/10.1021/acsapm.2c01774.
[8] F. Cuminet, S. Caillol, É. Dantras, É. Leclerc, S. Lemouzy, C. Totée, O. Guille, V. Ladmiral, Synthesis of a transesterification vitrimer activated by fluorine from an α,α-difluoro carboxylic acid and a diepoxy, Eur. Polym. J. 182 (2023) 111718–111726, https://doi.org/10.1016/j.eurpolymj.2022.111718.
[9] A. Roig, P. Hidalgo, X. Ramis, S. De la Flor, À. Serra, Vitrimeric epoxy-amine polyimine networks based on a renewable vanillin derivative, ACS Appl. Polym. Mater. 4 (2022) 9341–9350, https://doi.org/10.1021/acsapm.2c01604.
[10] P. Taynton, K. Yu, R.K. Shoemaker, Y. Jin, H.J. Qi, W. Zhang, Heat- or water-driven malleability in a highly recyclable covalent network polymer, Adv. Mater. 26 (2014) 3938–3942, https://doi.org/10.1002/adma.201400317.
[11] M. Ahmadi, A. Hanifpour, S. Ghiassinejad, E. van Ruymbeke, Polyolefins vitrimers: design principles and applications, Chem. Mater. 34 (2022) 10249–10271, https://doi.org/10.1021/acs.chemmater.2c02853.
[12] Y. Lu, F. Tournilhac, L. Liebler, Z. Guan, Making insoluble polymer networks malleable via olefin metathesis, J. Am. Chem. Soc. 134 (2012) 8424–8427, https://doi.org/10.1021/ja303356z.
[13] S. Shan, D. Mai, Y. Lin, A. Zhang, Self-healing, reprocessable, and degradable bio-based epoxy elastomer bearing aromatic disulfide bonds and its application in strain sensors, ACS Appl. Polym. Mater 3 (2021) 5115–5124, https://doi.org/10.1021/acsapm.1c00865.
[14] K. Chang, H. Jia, S. Gu, A transparent, highly stretchable, self-healing polyurethane based on disulfide bonds, Eur. Polym. J. 112 (2019) 822–831, https://doi.org/10.1016/j.eurpolymj.2018.11.005.

[15] J. Zheng, Z.M. Png, S.H. Ng, G.X. Tham, E. Ye, S.S. Goh, X.J. Loh, Z. Li, Vitrimers: current research trends and their emerging applications, Mater. Today 51 (2021) 586–625, https://doi.org/10.1016/j.mattod.2021.07.003.
[16] W. Alabiso, S. Schlögl, The impact of vitrimers of the industry of the future: chemistry, properties and sustainable forward-looking applications, Polymers. 12 (2020) 1660–1690, https://doi.org/10.3390/polym12081660.
[17] B. Steyrer, B. Busetti, G. Harakály, R. Liska, J. Stampfl, Hot lithography vs room temperature DLP 3D-printing of a dimethacrylate, Addit. Manuf. 21 (2018) 209–214, https://doi.org/10.1016/j.addma.2018.03.013.
[18] S.C. Ligon, R. Liska, J. Stampfl, M. Gurr, R. Mülhaupt, Polymers for 3D printing and customized additive manufacturing, Chem. Rev. 117 (2017) 10212–10290, https://doi.org/10.1021/acs.chemrev.7b00074.
[19] B.K. Kumar, T.J. Dickens, Dynamic bond exchangeable thermoset vitrimers in 3D-printing, J. Appl. Polym. Sci. 2 (2023) 53304–53317, https://doi.org/10.1002/app.53304.
[20] X. Wang, M. Jiang, Z. Zhou, J. Gou, D. Hui, 3D printing of polymer matrix composites: a review and prospective, Comp. Part B. 110 (2017) 442–458, https://doi.org/10.1016/j.compositesb.2016.11.034.
[21] E. Rossegger, R. Höller, D. Reisinger, J. Strasser, M. Fleisch, T. Griesser, S. Schögl, Digital light processing 3D printing with thiol-acrylate vitrimers, Polym. Chem. 12 (2021) 639–646, https://doi.org/10.1039/d0py01520b.
[22] M. Fei, T. Liu, B. Zhao, A. Otero, Y. Chang, J. Zhang, From glassy plastic to ductile elastomer: vegetable oil-based UV-curable vitrimers and their potential use in 3D printing, ACS Appl. Polym. Mater. 3 (2021) 2470–2479, https://doi.org/10.1021/acsapm.1c00063.
[23] E. Rossegger, R. Höller, D. Reisinger, M. Fleisch, J. Strasser, V. Wieser, T. Griesser, S. Schlögl, High resolution additive manufacturing with acrylate based vitrimers using organic phosphates as transesterification catalyst, Polymer 221 (2021) 123631–123638, https://doi.org/10.1016/j.polymer.2021.123631.
[24] Q. Shi, K. Yu, X. Kuang, X. Mu, C.K. Dunn, M.L. Dunn, T. Wang, H.J. Qi, Recyclable 3D printing of vitrimer epoxy, Mater. Horiz. 4 (2017) 598–608, https://doi.org/10.1039/c7mh00043j.
[25] J. Casado, O. Konuray, G. Benet, X. Fernández-Francos, J.M. Morancho, X. Ramis, Optimization and testing of hybrid 3D printing vitrimer resins, Polymers 14 (2022) 5102–5115, https://doi.org/10.3390/polym14235102.
[26] X. Li, R. Yu, Y. He, Y. Zhang, X. Yang, X. Zhao, W. Huang, Self-healing polyurethane elastomers based on a disulfide bond by digital light processing 3D printing, ACS Macro Lett. 8 (2019) 1511–1516, https://doi.org/10.1021/acsmacrolett.9b00766.
[27] J. Stouten, G.H.M. Schnelting, J. Hul, N. Sijstermans, K. Janssen, T. Darikwa, C. Ye, K. Loos, V.S.D. Voet, K.V. Bernaerts, Biobased photopolymer resin for 3D printing coating dynamic imine bonds for reprocessability, ACS Appl. Mater. Interfaces 15 (2023) 27110–27119, https://doi.org/10.1021/acsami.3c01669.
[28] J.A. Syrett, D.M. Haddleton, M.R. Whittaker, T.P. Davis, C. Boyer, Functional, star polymeric molecular carriers, built from biodegradable microgel/nanogel cores, Chem. Commun. 47 (2011) 1149–1451, https://doi.org/10.1039/c0cc04532b.
[29] K. Yamawake, M. Hayashi, The role of tertiary amines as internal catalysts for disulfide exchange in covalent adaptable networks, Polym. Chem. 14 (2023) 680–686, https://doi.org/10.1039/D2PY01406H.
[30] A. Ruiz de Luzuriaga, G. Solera, I. Azcarate-Ascasua, V. Boucher, H.-J. Grande, A. Rekondo, Chemical control of the aromatic disulfide exchange kinetics for tailor-made epoxy vitrimers, Polymer 239 (2022) 124457, https://doi.org/10.1016/j.polymer.2021.124457.
[31] A. Roig, M. Agizza, À. Serra, S. De la Flor, Disulfide vitrimeric materials base don cystamine and diepoxy eugenol as bio-based monomers, Eur. Polym. J. 194 (2023) 112185, https://doi.org/10.1016/j.eurpolymj.2023.112185.
[32] A. Kumar, L.A. Connal, Biobased transesterification vitrimersz, Macromol. Rapid Commun. 44 (2023) 2200892, https://doi.org/10.1002/marc202200892.
[33] Y. Tachibana, T. Baba, K. Kasuya, Enviromental biodegradation control of polymers by cleavage of disulfide bonds, Polym. Degrad. Stab. 137 (2017) 67–74, https://doi.org/10.1016/j.polymdegradstab. 2017.01.003.
[34] M. Arasa, X. Ramis, J.M. Salla, A. Mantecón, A. Serra, A study of the degradation of ester-modified epoxy resins obtained by cationic copolymerization of DGEBA with g-lactones initiated by rare earth triflates, Polym. Degrad. Stab. 92 (2007) 2214–2222, https://doi.org/10.1016/j.polymdegradstab. 2007.01.037.
[35] M. Chen, L. Zhou, Y. Wu, X. Zhao, Y. Zhang, Rapid stress relaxation and moderate temperature of malleability enabled by the synergy of disulfide metathesis and carboxylate transesterification in epoxy vitrimers, ACS Macro Lett. 8 (2019) 255–260, https://doi.org/10.1021/acsmacrolett.9b00015.
[36] O. Konuray, X. Fernández-Francos, X. Ramis, Structural design of CANs with fine-tunable relaxation properties: a theoretical framework based on network structure and kinetics modeling, Macromolecules 56 (2023) 4855–4873, https://doi.org/10.1021/acs.macromol.3c00482.
[37] M. Capelot, M. Unterlass, F. Tournilhac, L. Leibler, Catalytic control of the vitrimer glass transition, ACS Macro Lett. 1 (2012) 789–792, https://doi.org/10.1021/mz300239f.
[38] P. Yan, W. Zhao, X. Fu, Z. Liu, W. Kong, C. Zhou, J. Lei, Multifunctional polyurethane-vitrimers completely based on transcarbamoylation of carbamates: thermally-induced dual-shape memory effect and self-welding, RSC Adv. 7 (2017) 26858–26866, https://doi.org/10.1039/C7RA01711A.